

## Macromolecular Hydration Studied by Two-Dimensional Heteronuclear $^{13}\text{C}$ - $^1\text{H}$ Separation Spectroscopy†

S. Ganapathy,\* P. R. Rajamohanam,  
Siddharth S. Ray, A. B. Mandhare, and  
R. A. Mashelkar\*

National Chemical Laboratory, Pune 411 008, India

Received October 23, 1993

Revised Manuscript Received February 15, 1994

Macromolecular hydration has been a subject of considerable interest.<sup>1-3</sup> There is substantial evidence for the existence of ordered water structure near the aqueous-solid interface, and this water is known to behave quite differently from bulk water. The classification into "bound" and "free" states of water<sup>4,5</sup> has been widely accepted, and this has led to innumerable studies on water structure and dynamics.<sup>6-12</sup>

It has been recognized that proton NMR spectroscopy is a potentially powerful tool for studying the interaction of water with macromolecules.<sup>13,14</sup> However, in most dilute polymer solutions and gels, proton NMR is dominated by the bulk water signal.<sup>15</sup> This renders the direct study of water macromolecular association rather difficult. Refinement in NMR methodology has led to the application of one-dimensional solid-state methods, such as rare-spin  $^{13}\text{C}$  NMR,<sup>16,17</sup> in hydrated systems. Hydration response has been studied this way in synthetic polymers<sup>18,19</sup> and biopolymers.<sup>20-23</sup>

In this communication we show that the dynamic state of water and of the polymer can be studied by two-dimensional heteronuclear  $^{13}\text{C}$ - $^1\text{H}$  solid-state NMR spectroscopy. The technique is similar to that proposed by Spiess and co-workers.<sup>24</sup> By allowing proton evolution during incremented  $t_1$ , proton-carbon mixing during  $\tau_m$ , and a high-resolution carbon detection during  $t_2$ , a two-dimensional separation of carbon and proton spectral response is obtained. During  $t_1$ , a component of the precessing proton transverse magnetization is spin-locked along an applied rf field, and this modulates the intensity of the  $^{13}\text{C}$  resonance which participates in the magnetization transfer. This leads to an indirect detection of the proton spectrum along the  $F_1$  axis. High-resolution  $^{13}\text{C}$  detection is achieved by combining dipolar decoupling and magic angle sample spinning while the proton-carbon mixing is established by a matched Hartmann-Hahn<sup>25</sup> cross-polarization scheme. The dynamical state of the polymer and water is directly coded by observing the events during this mixing period. We have specifically synthesized and studied the hydration in the hydrophilic polymer hydrolyzed starch-*g*-poly(acrylonitrile) (HSPAN) and the LCST polymer poly(*N*-isopropylacrylamide) (PNIPAm).

We show in Figure 1A the two-dimensional carbon-proton spectral separation for dry unhydrated HSPAN, together with the  $F_1$  and  $F_2$  projections. Due to dipolar decoupling and magic angle spinning, distinct  $^{13}\text{C}$  sites in the pendant chains and the starch backbone are resolved and identified in the  $^{13}\text{C}$  spectrum. The cross-section through each resolved carbon resonance yields identical wide-line proton spectra. These are featureless Gaussians

of width 48 kHz in each case. Manifestation of the same broad-line proton spectrum at each carbon site shows that in this rigid phase pure polymer proton "spin diffusion" is very efficient and polarization is transferred to the individual carbons from polymer protons acting as a single thermodynamic reservoir.

The two-dimensional experiment on a hydrated HSPAN (0.4 g of water/g of polymer) leads to a  $^{13}\text{C}$ - $^1\text{H}$  spectral separation in a similar way. This is shown in Figure 1B, where the two-dimensional data were limited to 28 experiments due to experimental constraints. Unlike the dry polymer, the proton spectra obtained at the distinct carbon sites are clearly seen to be different in this hydrated polymer. A proton line exhibiting a broad and a very narrow component is separated at starch ( $\text{C}_1$ ,  $\text{C}_{2,3,5}$ ) and pendant ( $\text{CH}$ ,  $\text{CH}_2$ ) carbon resonance positions. For the carboxylate/amide ( $\text{COO}^-$ ,  $\text{CONH}_2$ ) carbons of the pendant chain, the two-dimensional separation essentially leads to a single Lorentzian proton line of width 4.5 kHz. While it is a formidable task to calculate these proton line shapes resulting from multispin dipolar interactions in the hydrated state, a characterization of the broad and narrow components in terms of line shape and line width is completely sufficient to unravel hydration details. This is done by an analysis of the  $t_1$  time domain response at each carbon, obtained from the 2-D data set  $[S(t_1, t_2)]$  that has been Fourier-transformed along  $t_2$ . The results are shown in Figure 2. Full details of the analysis are included in the figure caption.

For the starch  $\text{C}_1$  and  $\text{C}_{2,3,5}$  and the pendant  $\text{CH}/\text{CH}_2$ , the broad and narrow components of the 2-D separated proton line shapes are identified with polymer and water protons, respectively.<sup>27</sup> This identification is supported by our observations (spectra not shown) that the intensity of the narrow component changes in proportion with the amount of hydration water and with the isotopic dilution with  $\text{D}_2\text{O}$ . Similarly, it is found that under identical experimental conditions the  $\text{COO}^-/\text{CONH}_2$  carbon signal intensity is drastically reduced in the 2-D experiment for a 0.4 g/g  $\text{D}_2\text{O}$  (100%, Aldrich) hydrated polymer. Thus for these carbons, the single Lorentzian proton spectrum is mainly due to water, thus envisaging a direct interaction with the hydrated water at these sites.

In HSPAN, the carboxylate and amide groups of the pendant chains and the hydroxyl groups ( $\text{OH}$ ) of the starch backbone act as primary hydration sites.<sup>28</sup> Moreover, due to grafting, the pendant and starch units are spatially isolated. Consequently, the hydrated water protons at these units are isolated from one another as well. For the starch units there are two proton types, namely, water protons and the polymer protons (nonexchangeable  $\text{CH}$  and  $\text{CH}_2$  and exchangeable  $\text{OH}$ ).<sup>27</sup> The exchangeable hydroxyl protons may not be distinguishable from the hydration water at these sites due to rapid exchange. Similarly, pendant units comprise only two types of protons, namely, hydrogen-bonded water protons at the  $\text{COO}^-$  and  $\text{CONH}_2$  sites and the polymer protons ( $\text{CH}$ ,  $\text{CH}_2$ ). We also note that at the 0.4 g/g hydration level, there is no bulk water phase.<sup>28</sup>

The polymer protons and water protons constitute two separate proton pools that interact magnetically.<sup>7,14,20,29</sup> The protons in the polymer phase as well as the protons in the water phase have, at any time, a uniform spin temperature. The large dipolar width for the polymer component shows that within the polymer phase spin diffusion among the polymer protons will establish a common spin temperature. In the water phase, this is achieved by rapid chemical exchange, dominant at starch

\* To whom correspondence may be addressed.

† NCL Communication No. 5885.

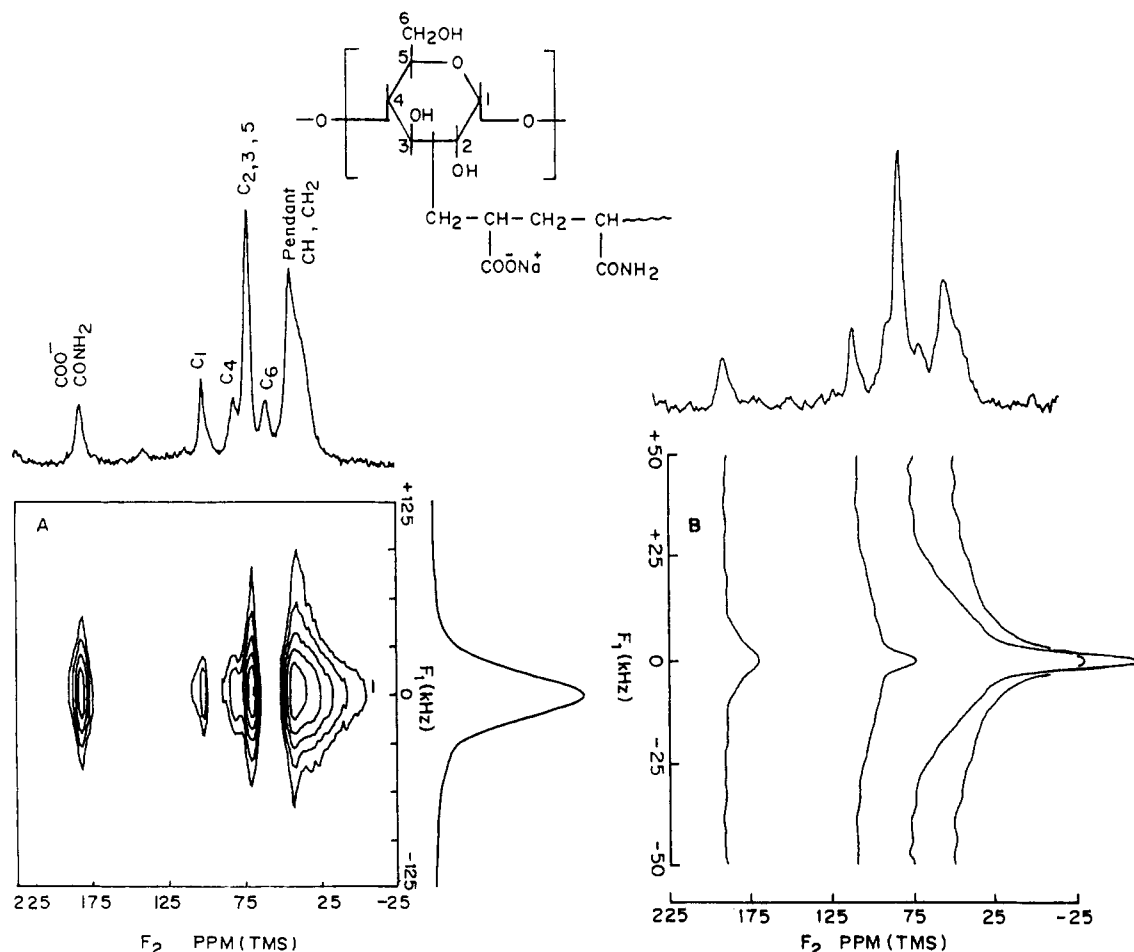


**Figure 1.** Two-dimensional heteronuclear  $^{13}\text{C}$ - $^1\text{H}$  separation for unhydrated dry (A) and 0.4 g/g (water/polymer) hydrated (B) hydrolyzed starch-g-poly(acrylonitrile) ( $T = 298\text{ K}$ ). The contours in A show the separation of the proton spectrum at each resolved carbon. For the dry polymer, cross-sections at each carbon in the repeat unit give rise to identical (in line shape and line width) wide-line proton spectra. Hence only the  $F_1$  projected proton wide-line spectrum is shown in A. For the hydrated polymer (B), the  $F_1$  cross-sections corresponding to different carbon resonances show distinct proton spectra. These spectra were obtained by extracting the submatrix columns at each carbon site and Fourier-transforming along  $F_1$ . The  $t_1$  increment is  $1\text{ }\mu\text{s}$  for A and  $10\text{ }\mu\text{s}$  for B, and the number of experiments is 26 for A and 28 for B. The number of scans is 400 for A and 480 for B. The cross-polarization mixing time for A is  $700\text{ }\mu\text{s}$  and for B is  $600\text{ }\mu\text{s}$ .

sites, or by mutual spin-spin interactions, which may be considered for the hydration water located at the less restricted  $\text{COO}^-$  and  $\text{CONH}_2$  sites. The longitudinal magnetization in each phase may therefore be considered to be uniform. The slow molecular mobility in the polymer phase and the rapid water motion in the water phase would suggest that the water phase acts as a relaxation sink for the polymer protons.<sup>29</sup> On the basis of earlier studies of biopolymer hydration, the cross-relaxation time for the diffusion of laboratory-frame magnetization from the polymer to water protons occurs in the tens of millisecond time scale.<sup>29</sup> To the best of our knowledge, no literature value of the spin diffusion time for the exchange of spin-locked magnetization between the polymer and water protons in a hydrated macromolecular system is available. In a separate experiment we have allowed complete dephasing of the rapidly decaying polymer component and spin-locked only the water component. Upon 2-D Fourier transformation, we see only the narrow water proton spectrum appearing along  $F_1$ . This is demonstrated in Figure 2a,b for the  $\text{C}_{2,3,5}$  of the starch backbone. Thus, practically no cross-relaxation between the polymer and water protons occurs during the Hartmann-Hahn cross-polarization period, and a bimodal heteronuclear  $^1\text{H}$ - $^{13}\text{C}$  cross-polarization transfer occurs from each of these distinct proton reservoirs to the nearby carbons.

The polymer protons in the starch backbone and pendant chains experience strong dipole-dipole interactions, occurring in the rigid polymer phase, giving rise to the Gaussian line shape for the broad polymer component ( $\Delta\nu \approx 25\text{ kHz}$ ). This width is however reduced from the rigid lattice value of  $48\text{ kHz}$ , noticed for the dry polymer, due to enhanced polymer segmental mobility upon hydration. For "bound" water molecules, intramolecular dipole-dipole interactions are averaged by the anisotropic water motions. This gives rise to the Lorentzian line shape for the water component, with a line width that is considerably smaller than that of the polymer component. It has been clearly observed that the water component is narrower at the starch sties ( $\Delta\nu \approx 400\text{ Hz}$ ) than at the pendant sites ( $4\text{--}5\text{ kHz}$ ), thus showing that water mobility is more restricted at the carboxylate and amide sites.<sup>30</sup> This is attributable to differences in the strength of the hydrogen bonds formed by water at these sites.<sup>31</sup>

The two-dimensional plot for a water-rich polymer, poly(*N*-isopropylacrylamide), is shown in Figure 3. This polymer is known to respond to water readily and undergo a thermoreversible volume phase transition at around  $305\text{ K}$  due to a lower critical solution temperature (LCST) phenomenon.<sup>32,33</sup> It exists in either of the two hydrated states, namely, an equilibrium-swollen state (below LCST) or a collapsed state (above LCST). For the equilibrium-swollen polymer, the two-dimensional experiment does

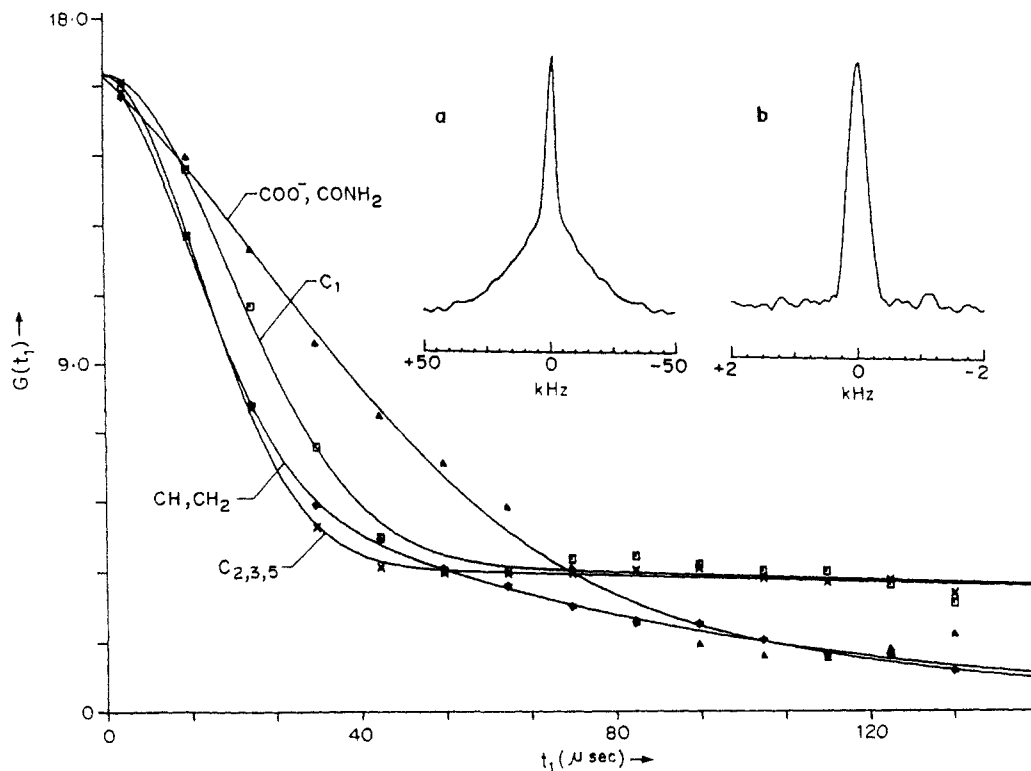


**Figure 2.** Time-domain response obtained from the 2-D data set of 0.4 g/g hydrated polymer after Fourier transformation along  $t_2$ . Various symbols denote experimental data points for the different carbons. The solid line has been calculated by fitting to the function  $I = I_L(0) \exp(-t_1/T_L) + I_G(0) \exp(-(t_1/T_G)^2)$ , where  $T_G$  and  $T_L$  represent the Gaussian and Lorentzian decay constants, respectively. The analysis yields the following values for  $T_G$  and  $T_L$ :  $C_1$ , 27.67 and 694.56  $\mu$ s;  $C_{2,3,5}$ , 21.21 and 784.31  $\mu$ s;  $CH, CH_2$ , 20.13 and 70.64  $\mu$ s. This corresponds to line widths for the Gaussian ( $C_1 = 19.2$  kHz,  $C_{2,3,5} = 25.04$  kHz,  $CH, CH_2 = 26.38$  kHz) and Lorentzian ( $C_1 = 458$  Hz,  $C_{2,3,5} = 406$  Hz,  $CH, CH_2 = 4.51$  kHz). For  $COO^-/CONH_2$ , analysis yields only a Lorentzian decay with  $T_L = 59.6$   $\mu$ s ( $\Delta\nu = 5.34$  kHz). The insert shows the proton spectra obtained by Fourier-transforming the  $t_1$  domain interferograms of  $C_{2,3,5}$ : (a) data obtained from 28 experiments using a  $t_1$  increment of 10  $\mu$ s; (b) data obtained from 24 experiments using a  $t_1$  increment of 125  $\mu$ s. The narrow proton resonance in b ( $\Delta\nu = 345$  Hz) is due to water (see text).

not lead to wide-line proton separation at the carbon sites. Instead, the cross-sections show isolated C-H correlations (A), thus giving a high-resolution polymer proton spectrum along the  $F_1$  axis (a). Noticeably, the dominant water resonance and the amide (CONH) peak in the  $^1H$  MAS spectrum (b) are not retrieved in the 2-D experiment. The hydration here far exceeds the bound-water limit<sup>35</sup> and allows a dominant bulk water phase to dictate the motional dynamics of the system. The polymer mobility has been enhanced to such an extent that proton-proton spin interactions within the polymer phase are greatly averaged. As shown elsewhere,<sup>34</sup> the resulting polymer proton line is inhomogeneously broadened, and MAS affords an efficient narrowing to allow proton chemical shift evolution during  $t_1$ . The water-induced polymer motions are clearly anisotropic, lest no correlation via cross-polarization would be observed. Water, due to its high dynamic state of exchange and rotational and translational mobility, is totally decoupled from the polymer system and is precluded from participating in the cross-polarization process.

The two-dimensional plot for the collapsed state of the polymer (B), however, leads to proton wide-line separation at each of the carbon resonances. The proton subspectra at each resolved carbon site are similar, characterized by a single Lorentzian of width  $\sim 8$  kHz. Since at 318 K the polymer is in the collapsed state, a significant amount of free water has been removed from the polymer matrix.<sup>34</sup> This noninteracting bulk water is essentially eliminated in the indirectly detected proton spectrum. A recent DSC study on this polymer has shown that above the LCST nearly all the water in the polymer is nonfreezing bound water.<sup>35</sup> The distinction of polymer and the bound-water

components is not readily forthcoming in (B), however. This is presumably due to the spectral overlap of the mobile polymer and more restricted water.

The 2-D experiments were performed on a Bruker MSL-300 FT-NMR spectrometer at the Larmor frequencies of 300.13 and 75.48 MHz for  $^1H$  and  $^{13}C$ , respectively. A  $(\pi/2)_{\phi_1}^I - (t_1/2) - (\pi)_{\phi_2}^S - (t_1/2) - (\tau_m)_{\phi_2, \phi_3}^{IS} - (t_2)_{R\phi}^I$  (relaxation delay) pulse sequence was used, where I and S denote  $^1H$  and  $^{13}C$  irradiation, respectively,  $\phi$ 's are the transmitter rf phases, and  $R\phi$  represents the receiver phase. The  $\pi$  pulse in the middle of the  $t_1$  period is not required when wide-line proton response is obtained. Quadrature detection in  $t_1$  was employed when chemical shift resolved proton spectral separation is obtained. Proton spin-temperature alternation and CYCLOPS during  $t_2$  were incorporated in a 16-step phase cycling. For cross-polarization mixing, a 40-kHz rf field was used on the  $^1H$  and  $^{13}C$  channels. A power mode calculation was employed. MAS was maintained at around 2.3 kHz. Other relevant 2-D parameters are included in the figure captions.

HSPAN and PNIPAm were synthesized in our laboratory as described elsewhere.<sup>34,36</sup> Hydrated HSPAN was prepared by controlled exposure of the polymer to water vapor in a humidity chamber. Hydrated PNIPAm was prepared by direct addition of a known amount of water to the polymer and subsequent equilibration for 4 days.

We have shown that macromolecular hydration can be conveniently studied by two-dimensional heteronuclear  $^{13}C$ - $^1H$  separation spectroscopy. The experiment offers considerable scope to study the dynamics of the polymer and that of water at the polymer-water interface. This has been demonstrated in water-poor hydrolyzed starch-

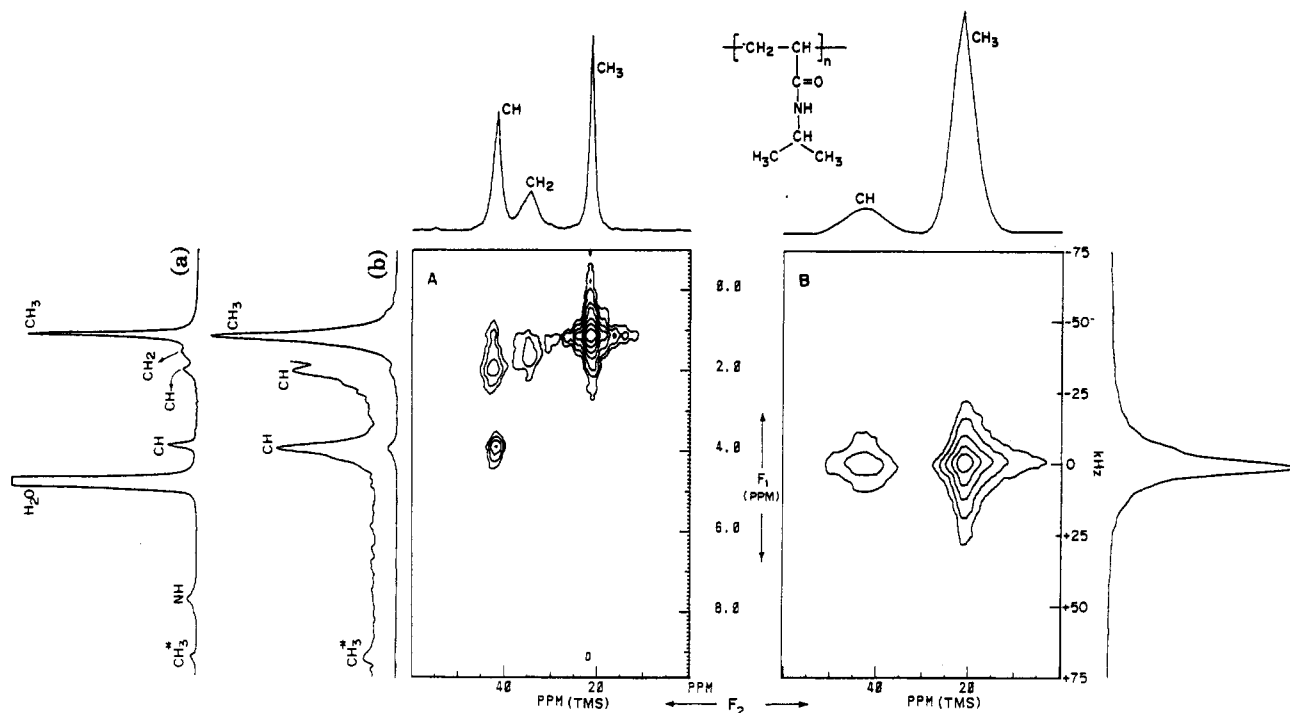


**Figure 3.** Two-dimensional heteronuclear  $^{13}\text{C}$ - $^1\text{H}$  separation for the LCST polymer poly(*N*-isopropylacrylamide) at 298 (A) and 323 K (B). Contour plots show the proton spectral response at each resolved carbon. At 298 K (A), cross-sections at the observed carbon positions give rise to distinct high-resolution proton spectra, correlating the carbon resonance with the dipolar coupled proton at the proton chemical shift. The sum of these proton subspectra leads to the  $F_1$  projection, as shown (a). The 1-D  $^1\text{H}$  MAS spectrum is also shown for comparison (b). The  $^1\text{H}$  sideband is marked with an asterisk. At 323 K, cross-sections at the observed carbon positions lead to identical (in line shape and line width) wide-line proton spectra. Hence only the  $F_1$  projected proton spectrum is shown in B. The absence of the  $\text{C}=\text{O}$  peak in A and B and the  $\text{CH}_2$  peak in B is due to motional effects of the polymer. The  $t_1$  increment is 125  $\mu\text{s}$  for A and 3.33  $\mu\text{s}$  for B, and the number of experiments is 90 for A and 64 for B. The number of scans is 880 for A and 400 for B. The cross-polarization mixing time for A is 2.5 ms and for B is 450  $\mu\text{s}$ .

*g*-poly(acrylonitrile) and in water-rich poly(*N*-isopropylacrylamide). Our studies pave the way for similar studies of hydrations of biopolymers such as collagen, DNA, etc.

## References and Notes

- Rupley, J. A.; Careri, G. *Adv. Protein Chem.* **1991**, *41*, 38.
- Bryant, R. G. *Stud. Phys. Theor. Chem.* **1988**, *38*, 683.
- In *Water in Polymers*; Rowland, S. P., Ed.; ACS Symposium Series 127; Washington, DC, 1980.
- Woessner, D. E.; Snowden, B. S., Jr. *J. Colloid Interface Sci.* **1970**, *34*, 290.
- Foster, K. R.; Resing, H. A.; Garroway, A. N. *Science* **1976**, *194*, 324.
- Symons, M. C. R. *Philos. Trans. R. Soc.* **1975**, B272, 13.
- Shirley, W. M.; Bryant, R. G. *J. Am. Chem. Soc.* **1982**, *104*, 2910.
- Kasturi, S. R. *Physiol. Chem. Phys. Med. NMR* **1985**, *17*, 387.
- Clore, G. M.; Bax, A.; Wingfield, P. T.; Gronenborn, A. M. *Biochemistry* **1990**, *29*, 5671.
- McBrierty, V. J.; Quinn, F. X.; Keely, C.; Wilson, A. C.; Friends, G. D. *Macromolecules* **1992**, *25*, 4281.
- Kubinec, M. G.; Wemmer, D. E. *J. Am. Chem. Soc.* **1992**, *114*, 8739.
- Otting, G.; Liepinsh, E.; Wuthrich, K. *Science* **1991**, *254*, 974.
- Berendsen, H. J. C. *J. Chem. Phys.* **1962**, *36*, 3297.
- Wise, W. B.; Pfeffer, P. E. *Macromolecules* **1987**, *20*, 1550.
- Maquet, J.; Theveneau, H.; Djabourov, M.; Leblond, J.; Papon, P. *Polymer* **1986**, *27*, 1103.
- Schaefer, J.; Stejskal, E. O. *J. Am. Chem. Soc.* **1976**, *98*, 1031.
- Voelkel, R. *Angew. Chem., Int. Ed. Engl.* **1988**, *27*, 1468.
- Terao, T.; Maeda, S.; Saika, A. *Macromolecules* **1983**, *16*, 1535.
- Ganapathy, S.; Chacko, V. P.; Bryant, R. G. *Macromolecules* **1986**, *19*, 1021.
- Jelinski, L. W.; Sullivan, C. E.; Torchia, D. A. *J. Magn. Reson.* **1980**, *41*, 133.
- Jackson, C. L.; Bryant, R. G. *Biochemistry* **1989**, *28*, 5024.
- Kennedy, S. D.; Bryant, R. G. *Biopolymers* **1990**, *29*, 1801.
- Gregory, R. B.; Gangoda, M.; Gilpin, R. K.; Su, W. *Biopolymers* **1993**, *33*, 513.
- Schmidt-Rohr, K.; Clauss, J.; Spiess, H. W. *Macromolecules* **1992**, *25*, 3273.
- Hartmann, S. R.; Hahn, E. L. *Phys. Rev.* **1962**, *128*, 2042.
- Rajamohan, P. R.; Badiger, M. V.; Ganapathy, S.; Mashelkar, R. A. *Macromolecules* **1991**, *24*, 1423.
- Tanner, S. F.; Hills, B. P.; Parker, R. J. *Chem. Soc., Faraday Trans.* **1991**, *87*, 2613.
- Rodehed, C.; Ranby, B. *J. Appl. Polym. Sci.* **1986**, *32*, 3309.
- Edzes, H. T.; Samulski, E. T. *Nature* **1977**, *256*, 521.
- Line-narrowing effects due to MAS ( $\nu_r = 2.3$  kHz) are negligible for the broad polymer component. For the more restricted water at  $\text{COO}^-/\text{CONH}_2$  sites, interactions within the tightly bound water molecules impart homogeneous broadening to the residual water line width, making it less amenable for narrowing by MAS. For the less restricted water at the hydroxyl sites, the water line may be considered to be inhomogeneously broadened, and MAS is effective in narrowing the water resonance. These are reflected in the width of water resonances indirectly detected in the 2-D experiment. (See also: Yesinowshi, J. P.; Echert, H.; Rossman, G. R. *J. Am. Chem. Soc.* **1988**, *110*, 1367. Brunner, E.; Freude, D.; Gerstein, B. C.; Pfeifer, H. *J. Magn. Reson.* **1990**, *90*, 90.)
- Vinogradov, S. N.; Linnell, R. H. *Hydrogen Bonding*; Van Nostrand Reinhold Co.: New York, 1970, p 121.
- Schild, H. G. *Prog. Polym. Sci.* **1992**, *17*, 163.
- Tokuhiro, T.; Amiya, T.; Mamada, A.; Tanaka, T. *Macromolecules* **1991**, *24*, 2936.
- Badiger, M. V.; Kulkarni, M. G.; Rajamohan, P. R.; Ganapathy, S.; Mashelkar, R. A. *Macromolecules* **1991**, *24*, 106.
- Dong, L. C.; Hoffman, A. S. *Proceedings of the International Symposium on Controlled Release of Bioactive Materials*, Controlled Release Society, Inc., **1990**, *17*, 116.
- Ganapathy, S.; Rajamohan, P. R.; Badiger, M. V.; Mashelkar, R. A. *New Polym. Mater.* **1990**, *2*, 205.